Nonlinearity and isotope effect in temporal evolution of mesoscopic structure during hydration of cement

S. Mazumder,[1,*] D. Sen,[1] J. Bahadur,[1] J. Klepp,[2,3] H. Rauch,[4,5] and José Teixeira[6]
[1]*Solid State Physics Division, Bhabha Atomic Research Centre, Mumbai 400085, India*
[2]*Atominstitut der Österreichischen Universitäten, A-1020 Wien, Austria*
[3]*Fakultät für Physik, Universität Wien, Boltzmanngasse 5, A-1090 Wien, Austria*
[4]*Atominstitut der Österreichischen Universitäten, A-1020 Wien, Austria*
[5]*Institut Laue-Langevin, BP 156, 38042 Grenoble Cedex 9, France*
[6]*Laboratoire Léon Brillouin, CEA-Saclay/CNRS, 91191 Gif-sur-Yvette Cedex, France*
(Received 31 May 2010; published 24 August 2010)

Though cement is a ubiquitous material with global production exceeding that of any other material of technological importance, the mechanism of its hydration and evolution of cement-water mixtures into gels of high compressive strength is poorly understood, despite extensive research over the past century. The present investigation, based on neutron-scattering measurements, aims at unraveling this enigma and outlines the evolution of the mesoscopic structure of the cement paste which exhibits temporal oscillations, strongly dependent on the scale of observation and on the medium of hydration (light or heavy water). While the formation of hydration products is synchronous for hydration with H_2O, the process is nonsynchronous for hydration with D_2O. The reason why morphological patterns of domains at different times look dissimilar, as seen before [S. Mazumder, D. Sen, A. K. Patra, S. A. Khadilkar, R. M. Cursetji, R. Loidl, M. Baron, and H. Rauch, Phys. Rev. Lett. **93**, 255704 (2004); Phys. Rev. B **72**, 224208 (2005)], for different hydration media emerges as a natural consequence of this finding. The present investigation also provides an explanation for disagreement with the hypothesis of dynamical scaling for hydration of cement with heavy water and is a step forward toward general understanding of hydration process.

DOI: 10.1103/PhysRevB.82.064203 PACS number(s): 64.75.−g, 61.43.Hv, 61.50.Ks

I. INTRODUCTION

The phenomenon of new phase formation is a representative example of first-order transition and dynamics of the transition is of immense interest as an example of a highly nonlinear process far from equilibrium. In accordance with the linear theory[1] of new phase formation, time (t) -dependent scattering function $S(\mathbf{q},t)$ is given by

$$S(\mathbf{q},t) = S(q,0)\exp[2t\alpha(q)],$$

where $\alpha(q)$ is the time-independent proportionality constant indicating temporal amplification of composition wave and q is the modulus of the scattering vector $\mathbf{q}$. The dependence of $S(\mathbf{q},t)$ on scalar q indicates the isotropic nature of the system. The dependence of $\alpha(q)$ on q is given by

$$\alpha(q) = Dq^2[1-(q/q_c)^2],$$

where D is the diffusion coefficient of species primarily responsible for new phase formation and q_c is a critical q such that $\alpha(q)$ maximizes at $q=q_c/\sqrt{2}$. In accordance to the linear theory, $S(\mathbf{q},t)$ increases monotonically for $q<q_c$ and a monotonic diminution to zero for $q>q_c$. For $q=q_c$, $S(\mathbf{q},t)$ is time invariant. In the limit $t\rightarrow 0$, new phase forming systems follow the linear theory.

At late stages, the dynamics of new phase formation is highly nonlinear process far from equilibrium. The new phase forming systems exhibit self-similar growth pattern with dilation symmetry, with time-dependent scale, and scaling phenomenon.[2] The phenomenon is indicative of the emergence of a morphological pattern of the domains at earlier times looking statistically similar to a pattern at later times apart from the global change in scale implied by the growth of time-dependent characteristic length scale $L(t)$—a measure of the time-dependent domain size of the new phase. In the past, extensive theoretical investigations,[2] based on spin-lattice models, on scaling phenomenon in Euclidean geometry with regular geometrical properties with spins occupying the cells of a regular Bravais lattice have been reported.[2]

The scaling hypothesis assumes the existence of a single characteristic length scale $L(t)$, such that the domain sizes and their spatial correlation are time invariant when the lengths are scaled by $L(t)$. For a system exhibiting dynamical scaling, it is only implicit that domains, very large in number for a conceivable macroscopic system, are in communication with each other such that they are scaled by the same characteristic length $L(t)$. This is a mystery indeed and deserves much closer experimental scrutiny.

Quantitatively, an isotropic system exhibiting dynamical scaling, the equal-time spatiotemporal composition modulation autocorrelation function $g(r,t)$, r denoting the spatial coordinate of the system, reflects the way in which the mean density of the medium varies as a function of distance from a given point, should exhibit the scaling form with time-dependent dilation symmetry $g(r,t)=f[r/L(t)]$. The scaling function $f[r/L(t)]$ is universal in the sense that it is independent of initial conditions and also on interactions as long as they are short ranged. However, form of $f(r/L(t))$ depends nontrivially on n, the number of components in the vector order-parameter field exhibiting the scaling behavior and d, the embedding dimension of the system. The Fourier transform of $g(r,t)$, the structure factor or scattering function

$S(q,t)$ for a d-dimensional Euclidean system, obeys simple-scaling ansatz at late times, $S(q,t)=L(t)^d F[qL(t)]$. It is important to note that the scaling hypothesis has not been proved, partially due to the strong nonlinear nature of the problem, conclusively except for some model systems. The need for investigations examining the extent and the nature of the validity of the dynamical scaling laws for different physical and geometrical conditions has already been discussed.[3–7] The validity of the dynamical scaling laws for new phase formation in the case of non-Euclidean fractal systems is still an open question. For a fractal system, the translational invariance of regular lattices is replaced by much weaker dilation invariance.

It has been observed[3,4] that the kinetics, of hydration of silicates with light and heavy water, are of nonlinear nature even at the initial time as realized by experiments. The scattering data could not be interpreted in terms of a linear theory[1] based on the diffusion equation. In the case of hydration of silicates with light water, the hydrating mass exhibits a mass fractal nature throughout hydration with the mass fractal dimension increasing with time and reaching a plateau. The second phase appears to grow with time initially. Subsequently, the domain size of the second phase saturates. It has also been demonstrated that light water hydration of silicates exhibits a scaling phenomenon for a characteristic length with a different measure. The exhibition of scaling phenomenon for non-Euclidean geometry has been reported. The temporal behavior of the characteristic length has been observed to be far from a power law.

For a fractal cluster with fractal dimension D_f, embedding Euclidean dimension d, time-dependent lower cutoff $l_1(t)$ and time-dependent upper cutoff $l_2(t)$, the interfacial area A, and total mass M are given[8] by $A(t)\sim[l_1(t)^{d-1}[l_2(t)/l_1(t)]^{D_f}$ and $M(t)\sim[l_1(t)^d[l_2(t)/l_1(t)]^{D_f}$, respectively.

In the time period where fractal dimension is increasing, for hydration of cement with heavy and light water, it can inferred that hydrating mass is increasing with time. Question remains about the time period where fractal dimension is constant or decreasing with time as hydrating mass cannot decrease with time. Further, incomprehensible nature of nonlinearity[3,4,6] for hydration of cement with heavy and light water indicates that hydration of cementitious material is far from being understood and deserve intense investigation. The present paper is a step in that direction.

Cement, steel and silicon are the three most important materials of technological importance but cement happens to be the one most widely used. The total world consumption of cement in 2008 was about 2.5 billion metric tons almost double of that of steel. Portland cement, commonly used in construction industry and in nuclear energy program for immobilization of nonheat-generating low-level radioactive waste, is a composite material consisting of fine grains of tricalcium silicate, $3CaO\cdot SiO_2$ (abbreviation C_3S; approximate mass percentage range 60–80 %) along with minor constituents such as dicalcium silicate, tricalcium aluminate, tetracalcium iron aluminate, etc. As the major constituent of Portland cement, C_3S can be used as a model for hydration of cement.

Investigation[9] on cement, a geopolymer, is more than a century old, yet the understanding of the mechanism by which cement-water mixtures turn into gels, rendering the requisite rigidity and compressive strength, remains far from being understood. The complexity arises mainly due to poor understanding of the hydration kinetics and physical nature of the hydration products. The present investigation aims to improve our understanding of the hydration process by outlining the temporal evolution of the mesoscopic structure encountered during hydration. Present findings also provide us an insight into the process of gelation.

On mixing cement and water, a complex series of hydration reactions[10] take place of which the main products are an amorphous calcium-silicate-hydrate (C-S-H) gel-like structure and crystalline calcium hydroxide. The mesoscopic structure of C-S-H gel determines the desirable properties of hardened cement. To elucidate the microscopic structure of the C-S-H gel, many models[11–16] have been proposed. The investigations,[3,4,6] based on small-angle neutron scattering (SANS), on continuous temporal evolution of mesoscopic structure during hydration of cement are recent. Small-angle scattering (SAS) technique can elucidate mesoscopic structure in the length scale of 10^2–10^4 Å and is an ideal probe for time-resolved structural investigation on C-S-H gel. Both neutrons and x rays are used as probing radiation for SAS investigations. Neutrons as probe have an advantage over x rays owing to their considerably higher penetration power. Therefore, relatively larger sample volume, representative of the bulk material in all essential properties, can be examined by neutron scattering. Neutrons are not invasive and they scatter very effectively from hydrogen-bearing materials such as those found in hydrated cements.

Small-angle x-ray[17] scattering (SAXS) and[18] SANS studies have demonstrated the fractal morphology of C-S-H gel. Further, SAXS investigations have demonstrated[17,19] that C-S-H gel undergoes transition from a ramified to a relatively more compact structure. However, examinations, involving continuous monitoring of temporal evolution of mesoscopic structure during hydration of cement with light water (H_2O) and heavy water (D_2O), have been reported[3,4,6,7] only recently. In these studies, observations on temporal evolution were restricted to a maximum time of 5 h only.

The hydration of cement with H_2O and D_2O is expected to be quite similar except for kinetics. However, some incomprehensible contrasting behavior has been observed[3,4] in the case of hydration of cement with D_2O as far as the kinetics of new phase formation is concerned. The domain size of the density fluctuations increases for a while in the beginning and appears to decrease to a lower limit subsequently. In the case of hydration of cement with D_2O, the mesoscopic structure of the hydrating mass undergoes a transition from mass fractal to surface fractal and then again to a mass fractal nature. A calorimetric investigation[20] indicates hydration of cement with D_2O is sluggish in comparison with that with H_2O. A conclusive reason for the aforementioned facts remains unknown to date.

The dynamics of new phase formation for hydration of cement exhibits nonlinearity[3,4,6] of incomprehensible nature even in the very initial stages of hydration. Isothermal heat-liberation rate has also been observed[21,22] to be highly nonlinear with time and somewhat oscillatory for several hours

during hydration. The above two facts call for outlining the temporal evolution of the mesoscopic structure encountered during hydration of cement. The observed[3,4,20] contrasting behavior evidenced from scattering experiments[3,4] and also from calorimetric measurements,[20] of hydration of cement with H_2O and D_2O, also call for examination of the hydration behaviors with both H_2O and D_2O.

II. EXPERIMENT

Pure powder specimens of C_3S were mixed with D_2O and double-distilled H_2O at varying w/c to obtain a pastelike mass. For D_2O hydrating specimens, $w/c=x$ actually corresponds to $w/c=x^*$ (20/18) to maintain same molar ratio of water and cement as in H_2O hydrating specimens with $w/c=x$. C-S-H gel is known[13–15] to have fractal mesoscopic structure in the length scale 10^2-10^3 Å. Preliminary measurements with a medium resolution SANS facility[23] indicated the possibility of existence of inhomogeneities larger than 10^3 Å. So SANS measurements were carried out with ultra-SANS (USANS) facility[24] at ILL, France. For scattering measurements, approximately 0.08 ml of the paste was spread in a circular hole of diameter 10 mm on a cadmium sheet of 1.0 mm thickness. Neutrons with wavelength $\lambda=1.92$ Å were used for USANS measurements. The scattered intensities, corrected for background and primary beam geometry, were recorded as a function of q. For background, measurements have been carried out at about $q=10^{-2}$ Å^{-1}. Background was relatively higher but insignificantly smaller in comparison to the scattering signal of interest for H_2O hydrating specimens. At the outset, it was inferred that hydrating specimens are isotropic in nature and so is the $S(q,t)$.[25]

Having observed linear decrease in $\ln[S(q,t)]$ versus $\ln(q)$ in the q range $0.00025-0.001$ Å^{-1}, it was considered worth extending the scattering measurements for larger q values using a conventional pinhole collimation SANS instrument PAXE at LLB, France. Measurements are performed with a monochromatic beam ($4<\lambda<25$ Å) with ($\Delta\lambda/\lambda$) is 10%. For measurements with PAXE, freshly prepared paste was spread in 1-mm-thick spacer placed between two circular quartz plates. The diameter of the specimens was 10 mm.

III. DATA INTERPRETATION AND DISCUSSION

The hydration reaction of C_3S can be written as

$$3\mathrm{CaO}\cdot\mathrm{SiO_2}+(3+y-x)\mathrm{H_2O}\rightarrow(\mathrm{CaO})_x(\mathrm{SiO_2})\cdot(\mathrm{H_2O})_y+(3-x)\mathrm{Ca(OH)_2},$$

where x is bounded by $0\le x\le 3$ and y is bounded on one side, i.e., $y\ge 0$. $x=3$ indicates hydration of C_3S without formation of $Ca(OH)_2$. Whether x varies with time is hitherto unknown. The product $(CaO)_x(SiO_2)\cdot(H_2O)_y$ (abbreviated as C-S-H, wherein hyphens indicate variable stoichiometry) is calcium silicate hydrate—a colloidal gel-like material. The other product is crystalline calcium hydroxide $Ca(OH)_2$. The gel constitutes about 60–70 volume percentage of the fully hydrated cement paste which is a composite wherein unreacted cement powder and $Ca(OH)_2$ crystals are embedded.

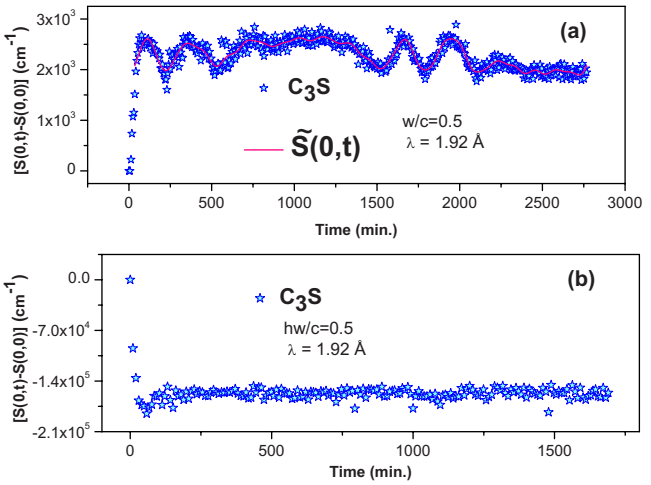

FIG. 1. (Color online) (a) Temporal evolution of $S(0,t)$ for H_2O hydrating C_3S with $w/c=0.5$. Red (online) solid line represents $\tilde{S}(0,t)$ composed of linear sum of 25 dominant frequencies in $S(0,t)$. (b) Temporal evolution of $S(0,t)$ for D_2O hydrating C_3S with $w/c=0.5$. Statistical error bars are smaller than the respective symbol sizes.

Because of the amorphous nature of C-S-H, the hydrated products unlike many crystalline systems are isotropic in nature and so is the scattering function $S(q,t)$ with q [$=4\pi(\sin\theta)/\lambda$, 2θ being the scattering angle and $\mathbf{q}$ being the scattering vector with $q=|\mathbf{q}|$].

Figure 1 depicts the temporal evolution of $S(q=0,t)$, a measure of total scattering length density has been recorded in absolute scale using USANS facility, for light and heavy water hydrating C_3S with water/cement ratio $(w/c)=0.5$ as shown in Figs. 1(a) and 1(b), respectively. It is evident from Fig. 1(a) that for H_2O hydrating C_3S, $S(q=0,t)$ oscillates (with periods of apparent silence in between) with time, albeit with nonregular periodicity. The oscillations have two different time scales. In shorter time scale, oscillations repeat after a gap of about 4 h but cease to exist for considerable time after the second oscillation. While on the longer time scale, oscillations repeat after a gap of about 25 h. A self-replicating pattern is observed for $S(q=0,t)$.

For a system of polydisperse population of inhomogeneities, with degree of polydispersity (m), $S(0,t)$ is given by

$$S(0,t)=\sum_{i=1}^{m}\tau_i(t)V_i^2(t)\rho_i^2(t)=\sum_{i=1}^{m}\tau_i(t)\zeta_i^2(t),$$

where the subscripted quantities τ_i, V_i, ρ_i, and ζ_i $(=V_i\rho_i)$ are, respectively, the number density, volume, scattering length density, and total scattering length integrated over volume of the ith type of inhomogeneity. An inhomogeneity is defined by the uniform scattering length density over its volume. It is important to note that $S(0,t)$ has parabolic dependence on ζ.

The oscillatory nature of $S(0,t)$ is indicative of the fact that there are competing factors for temporal evolution of $S(0,t)$—some causing decay and others causing growth of $S(0,t)$ with time resulting in nonmonotonic temporal evolution of $S(0,t)$. To appreciate the oscillatory nature of $S(0,t)$

and also to interpret scattering data depicted in Fig. 1, three model calculations (Model Calculations I–III in Appendix) for hydration of cement have been considered.

It is evident from the model calculations (Model Calculations I and III in Appendix) that for hydration of cement with H_2O, $S(0,t)$ increases with time for the time period when $Ca(OH)_2$ formation is significant and C-S-H phase is water rich. There are many other nondominant ongoing processes, as discussed (Model Calculations I and III in Appendix), such as domain splitting as well as agglomeration of domains of water-rich C-S-H sol. For hydration of cement with H_2O, $S(0,t)$ can decrease with time because of factors such as: (i) the time period over which $Ca(OH)_2$ formation is insignificant; (ii) the time period when C-S-H gel is cement rich with positive scattering length density even when $Ca(OH)_2$ formation is significant; and (iii) domain splitting of C-S-H gel, with positive scattering length densities of the split domains, as discussed (Model Calculations I in Appendix), could also be a contributing factor.

We put forward a conjecture for the change in course of the reaction responsible for nonmonotonic growth of $S(0,t)$ in the case of hydration of cement with H_2O. Cement particles in contact with H_2O initially form water-rich C-S-H sol and $Ca(OH)_2$ causing the growth of $S(0,t)$ principally. After sometime depending upon w/c, the sol in contact with cement particles transforms into cement-rich C-S-H gel primarily causing the decay of $S(0,t)$. Maxima of $S(0,t)$ are signatures of sol-to-gel transition. It is surmised that C-S-H gel is forming a protective layer on unreacted part of a cement grain upto a certain time. At some stage, the protective hydration layer is ruptured causing the spurt of growth of fresh hydration products from unhydrated cement surfaces leading to resumption of growth of $S(0,t)$. The latter process is somewhat repetitive. Periodic exposure of the unhydrated surface to free water leads to periodic growth of $S(0,t)$. It is worth noting that the mesoscopic structure of the gel changes with time enabling the exposure of unhydrated surfaces to free water. It is important to note that temporal evolution of heat evolution rate for hydration of cement is also oscillatory[20–22] in nature, but the nature of the oscillations and temporal variation are of different nature from those observed in variation in $S(0,t)$ with t.

Based on heat-liberation rate as measured with conduction calorimeter during hydration of cement with H_2O, it has been generally accepted[19–22,26] that hydration follows five broad stages, viz, (i) preinduction period having initial short-lived fast reaction giving off a burst of heat, (ii) induction period, lasting a few hours, during which only small quantities of heat are given off, (iii) acceleratory period, in which the main reaction first begins to occur rapidly. In this period renewed exothermic reaction occurs and increasing amount of heat are given off, (iv) deceleration period, a period of reaction at a decreasing rate after ~ 12 h and finally (v) a slow continuous reaction with the rate gradually decreasing after about one day.

But it is evident from the scattering measurement on hydration of cement with H_2O that temporal evolution of mesoscopic structure during hydration follows a much complex pattern and no inference can be drawn about the five broad stages, as inferred from the calorimetric measurement, of the reaction. It is only a conjecture that the hydration product formed on C_3S particles acts as a barrier hindering the migration of water to the unreacted surface. Subsequently, either cement-rich C-S-H phase undergoes changes such that permeability through the layer increases significantly or there is rupture of the layer at various stages causing renewed hydration reaction leading to formation of water-rich C-S-H sol as evident from the oscillatory behavior of $S(0,t)$ with time. The various possibilities for growth and decay of $S(0,t)$ have been discussed (Model Calculations I–III in Appendix).

In earlier experiments[3,4] for hydration of cement with H_2O, it has been observed that for the initial few (2–3) h, sizes of inhomogeneities grow with time and finally reach a plateau. Further, the hydration matrix has also been observed, in the length scale 10^3-10^4 Å (LS1), to be mass fractal with fractal dimension increasing with time initially and reaching a plateau. Temporal evolution of square of the linear dimension of the inhomogeneity mimics the trend of the temporal evolution of the fractal dimension. In the large time limit, the temporally evolving system exhibits self-similar growth pattern with dilation symmetry and with the scaling phenomenon.[2] In view of aforementioned observations, we can conclude that for hydration of cement with H_2O, water-rich mass fractal C-S-H sol and crystalline $Ca(OH)_2$ are formed initially. $Ca(OH)_2$ phase is a minor phase and the fractal structure pertains to major C-S-H phase. Both the fractal dimension and linear dimension of mass fractal C-S-H phase grow with time. The initial increase in mass fractal dimension with time reflects the transition from a ramified and porous structure to a relatively more compact homogeneous solid matrix by the processes of interlinking and space filling of the disjoint initial network with C-S-H phase and $Ca(OH)_2$. This observation also explains the increasing compressive strength[27] of hydrated cement with time. As system exhibits dynamical scaling phenomenon, ratio of linear sizes of $Ca(OH)_2$ crystallite, and C-S-H phase must be constant with time indicating the synchronous formation of $Ca(OH)_2$ and C-S-H throughout the hydration of cement. At a later stage, depending upon w/c, the water-rich C-S-H sol in contact with cement particles transforms into cement-rich C-S-H gel with mass fractal morphology. Mass fractal dimension and linear dimension of C-S-H gel both grow with time for sometime and reach a plateau.

A Monte Carlo simulation, for embedding Euclidean dimension of 2, corroborates[7] well with the trend of the observed, for real systems with embedding Euclidean dimension of 3, temporal evolution of fractal dimension and linear dimension of the inhomogeneity for hydration of cement with H_2O. But no conclusion could be drawn, at this stage, about temporal evolution of fractal dimension and the linear dimension of C-S-H gel beyond 3 h of mixing of cement and water because of lack of experimental observations.

To identify the periodic component in the temporal evolution of $S(0,t)$, it has been broken into cosine and sine waves. It has been noticed that $S(0,t)$ is composed predominantly of cosine and sine waves of well-defined frequencies such as 0.00227, 0.02043, 0.00681, 0.01589, and 0.0227 min^{-1} with decreasing order of significance.

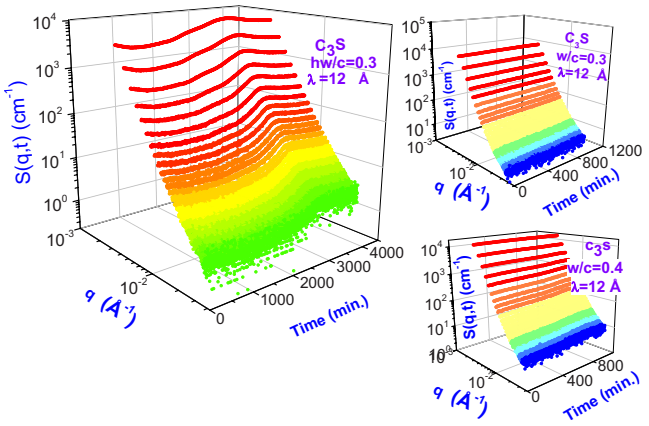

FIG. 2. (Color online) Temporal evolution of $S(q,t)$ for H_2O hydrating C_3S with $w/c=0.3$ and $w/c=0.4$; and for D_2O hydrating C_3S with $w/c=0.3$. Statistical error bars are smaller than the respective symbol sizes.

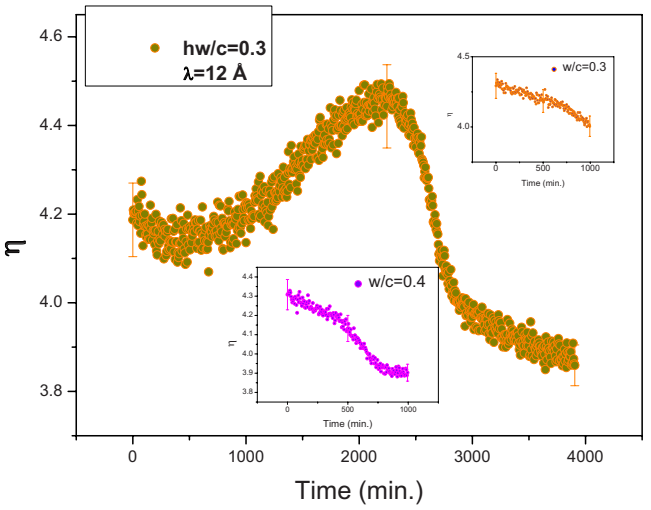

FIG. 3. (Color online) Temporal evolution of $\eta(t)$ associated with power-law scattering, as estimated from $\ln[S(q,t)]$ vs $\ln(q)$ in the q range 0.00423–0.01659 $Å^{-1}$ for various H_2O and D_2O hydrating specimens. Statistical error bars are marked at some discrete points only.

The red (online) solid line in Fig. 1 represents $\tilde{S}(0,t)$, the approximate $S(0,t)$, composed of 25 dominant cosines and sines of different frequencies, where $\tilde{S}(0,t)=\frac{a_0}{2}+\Sigma_{n=1}^{25}[a_n\cos(n\omega t)+b_n\sin(n\omega t)]$ with $\omega=0.00227$ min^{-1}. But we are not in a position to ascribe cyclic physicochemical processes responsible for the observation of aforementioned well-defined frequencies.

Considering the fact that hydrogen bond may be playing some important role in hydration kinetics and having observed[3,4,6] sharp contrasting features of temporal evolution of mesoscopic structure during hydration of silicates and sulphates with H_2O and D_2O, it was worth considering to repeat the scattering experiments to measure temporal evolution of $S(0,t)$ for hydration of cement with D_2O as it is known[28] that hydrogen bond with deuterium is slightly stronger than the one involving ordinary hydrogen. Further, lifetime of hydrogen bond involving D is longer vis-à-vis that involving H because the liberation motions perpendicular to the bond direction have smaller amplitude for D than that for H because of difference of masses. As far as chemistry is concerned, the hydration of cement with H_2O and D_2O is expected to be quite similar except for kinetics as diffusion of D_2O is somewhat sluggish because of its heavier molecular mass vis-à-vis H_2O. It is important to note that based on heat liberation rate as measured with conduction calorimeter during hydration of cement with H_2O and D_2O, it was inferred[20] earlier that induction period is delayed considerably and that the time corresponding to maximum heat evolution rate is also reduced considerably when D_2O is used for hydration. Apart from these two major differences, there is a gross similarity as far as the calorimetric measurements are concerned between hydration of cement with H_2O and D_2O. The total integrated heat output values were similar when either H_2O or D_2O were used for hydration.

The observations from scattering experiments on D_2O hydrating C_3S will be dealt with now. Figure 1(b) depicts the temporal evolution of $S(0,t)$ for D_2O hydrating C_3S with $w/c=0.5$. It is evident from Fig. 1(b) that $S(0,t)$ here has a simplistic variation and is grossly different vis-à-vis that observed for hydration of cement with H_2O. $S(0,t)$ decreases initially with time, reaching a minimum at about 55 min and then increases marginally and finally reaches a constant value barring few minor oscillations.

From the discussions (Model Calculations II.i in Appendix), it can be concluded that hydration reaction is slow, vis-à-vis with one with H_2O, upto 55 min. No conclusion can be drawn regarding the extent of formation of $Ca(OD)_2$. Increase in $S(0,t)$ with time, in the case of hydration of cement with D_2O, can be understood from the discussion (Model Calculations II.iii.F in Appendix).

In earlier experiments[3,4] for hydration of cement with D_2O, it has been observed that inhomogeneities grow in the beginning for a very short time and subsequently shrink with time. Temporal evolution of the mesoscopic structure in the length scale 10^3–10^4 Å have indicated that hydrating mass undergoes transition from mass fractal to surface fractal and finally again to mass fractal. Increase in mass fractal dimension indicates decrease in ramification and resulting finally in a solid core with increasing hydration time and a transition from mass fractal to surface fractal morphology. For hydration of cement with D_2O, no agreement has been observed with the dynamical scaling hypothesis. But these observations are valid for hydration time less than 5 h.

In view of aforementioned observations, we can conclude that for hydration of cement with D_2O, mass fractal calcium silicate deuterate (C-S-D) gel is formed initially. The pace of the reaction is slow. No conclusion can be drawn about the formation of $Ca(OD)_2$ at that stage. Both the fractal dimension and linear dimension of mass fractal C-S-D gel grow with time at the beginning. Later, when unreacted C_3S and D_2O are depleted considerably, reaction progresses with negligible amount of C-S-D and relatively large amount of $Ca(OD)_2$. At this stage mass reorganization in C-S-D gel takes place such that consolidation of gel occurs resulting into reduction in size associated with increasing fractal dimension attaining Euclidean-type topographical feature. The

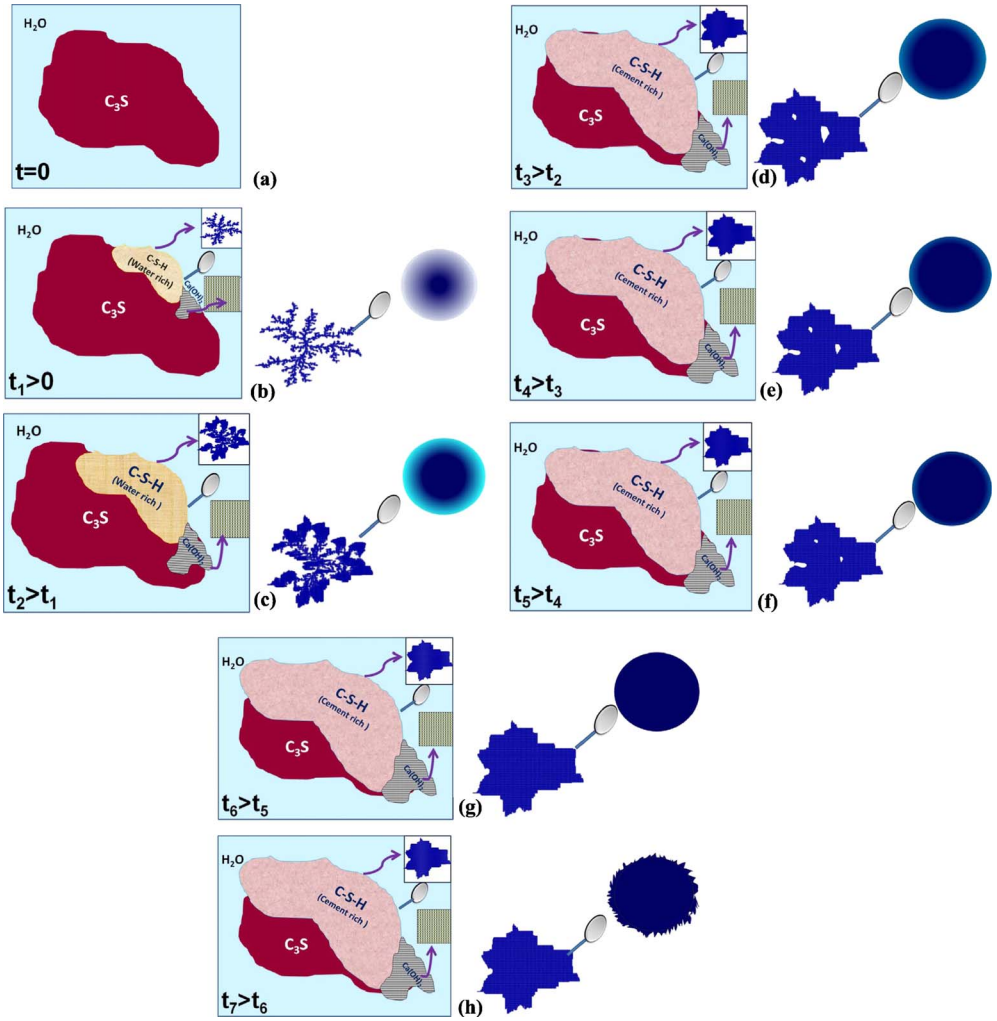

FIG. 4. (Color online) A schematic illustrating the mesoscopic structural evolution of cement hydrating with light water. LS1 and LS2 represent length scales 10^3-10^4 Å and 10^2-10^3 Å, respectively. (a) Depiction of initial state—a cement particle in contact with H_2O. (b) Initiation of hydration reaction forming water-rich C-S-H sol and crystalline $Ca(OH)_2$. Sol has mass fractal morphology in LS1. In LS2, sol has diffuse interface. (c) Growth of sol and $Ca(OH)_2$ follows dynamical scaling hypothesis implying growth with ratio of their increasing linear dimensions constant. In LS1, sol has increased mass fractal dimension, indicating transition from a ramified porous structure to a relatively more compact matrix. In LS2, sol has reduced diffuse interface. (d) Transition of sol phase to cement rich C-S-H gel phase occurs for first time at about 73 min for $w/c=0.5$. Growth of gel and $Ca(OH)_2$ follows dynamical scaling hypothesis. In LS1, gel has further increased mass fractal dimension, indicating transition to a more compact matrix. In LS2, gel has reduced diffuse interface. (e) Growth of gel and $Ca(OH)_2$ follows dynamical scaling hypothesis. In LS1, gel has further increased mass fractal dimension, indicating transition to a further compact matrix. In LS2, gel has reduced diffuse interface. (f) Linear dimensions of C-S-H gel and $Ca(OH)_2$ reach a plateau after about 150 min—so is for mass fractal dimension of gel in LS1 with the maximum attained value less than 3. This stage continues up to about 300 min. In LS2, gel has reduced diffuse interface. (g) At about 665 min, it is presumed that linear dimensions of gel and $Ca(OH)_2$ remain unchanged. In LS1, mass fractal dimension of gel also remains unchanged with the maximum attained value less than 3. In LS2, gel has sharp interface. (h) Beyond 665 min, in LS2, gel has surface fractal morphology.

hydrated gel attains uniform internal density with outer surface showing self-similar geometric properties. Negligible amount of C-S-D that forms, gets deposited on Euclidean-type gel leading into surface fractal-like morphology. Overall contraction of the gel and deposition on surface of the gel continues leading to formation of a mass fractal structure with a solid core. The question remains about why scaling is observed in hydration with H_2O but not with D_2O. It has been established[3,4] that for hydration with D_2O, the hydrating mass changes topographically with time unlike in the case of hydration with H_2O. In the beginning, the hydrating mass is ramified throughout the volume but the degree of ramification decreases with time. Then the mass transforms into objects with uniform internal density of unramified core with ramified outer surface exhibiting self-similar geometric properties. Later the ramified surface grows into ramified volume—the degree of ramification increasing with time. This topographical change in the hydrating mass as a function of time is a plausible explanation why scaling is not observed in the case of hydration with D_2O. Unlike in the case of H_2O, hydration with D_2O shows a formation rate of C-S-D and $Ca(OD)_2$ that varies differently with time. This is

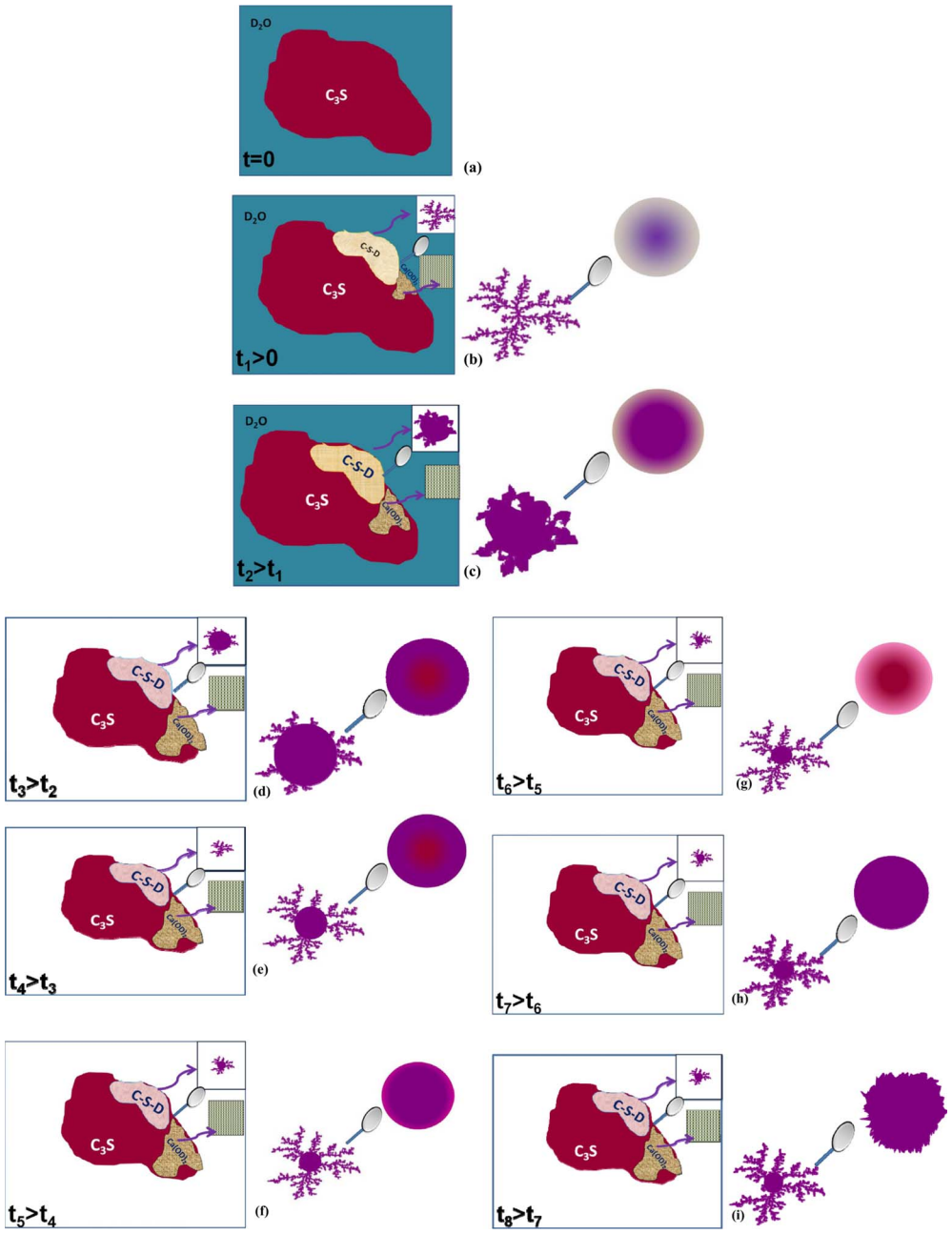

FIG. 5. (Color online) A schematic illustrating the mesoscopic structural evolution of cement hydrating with heavy water. LS1 and LS2 represent length scales 10^3-10^4 Å and 10^2-10^3 Å, respectively. (a) Depiction of initial state—a cement particle in contact with D_2O. (b) Initiation of hydration reaction forming C-S-D gel and crystalline $Ca(OD)_2$. Gel has mass fractal morphology in LS1. In LS2, gel has diffuse interface. (c) Growth of gel and $Ca(OD)_2$ continues without maintaining ratio of their increasing linear dimensions constant. Growth of linear dimension of gel continues for about 30 min for specimen with $hw/c=0.3$. In LS1, gel has increased mass fractal dimension. Increase in mass fractal dimension continues for about 65 min for hydrating specimen with $hw/c=0.3$. In LS2, gel has reduced diffuse interface. (d) Consolidation of gel occurs resulting into reduction in linear dimension. In LS1, gel has uniform internal density with surface fractal morphology in the time window 39–102 min. In LS2, gel has further reduced diffuse interface. (e) Consolidation of gel continues resulting into further reduction in linear dimension up to about 156 min. Reaction progresses with production of negligible amount of C-S-D and relatively large amount of $Ca(OD)_2$. In LS1, gel transforms into a mass fractal object beyond ~102 min. In LS2, gel has reduced diffuse interface. (f) Beyond 156 min, consolidation of gel is complete and linear dimension of gel attains a constant value. In LS1, mass fractal dimension of gel also reaches a constant value of ~2.45 after about 156 min. In LS2, reduction in diffuse interface of gel continues up to about 355 min. (g) In LS2, beyond 355 min, diffuse interface starts growing and growth continues up to about 2218 min. (h) In LS2, beyond 2218 min, diffuse interface starts shrinking to attain a sharp interface at about 2871 min. (i) In LS2, beyond 2871 min gel interface attains a surface fractal morphology.

another reason why scaling is not observed in the case of hydration of cement with D_2O. In fact, we have not come across any scattering experiment where scaling has been observed despite the topographical change in the second phase with time.

Previous time-resolved experiments,[3,4] with hydration times not exceeding 5 h, to investigate the temporal evolution of morphological features, in the length scale 10^3-10^4 Å, of hydrated gel C-S-H and C-S-D have indicated that for hydration of cement with H_2O, topographical mesoscopic structure could not be described in terms of classical porous medium with a well-defined specific inner surface. The mesoscopic structure is that of a mass fractal initially. Fractal dimension increases with time and reaches a plateau after about 150 min with the maximum attained value less than 3. Temporal evolution of square of the linear dimension of the inhomogeneity mimics the trend of the temporal evolution of the fractal dimension. In the large time limit, the temporally evolving systems obey dynamical scaling hypothesis. But, for hydration with D_2O, no agreement has been observed[3,4] with the dynamical scaling hypothesis. These observations are valid for hydration times less than 5 h.

Figure 2 depicts the temporal evolution of $S(q,t)$, measured with PAXE, for H_2O hydrating C_3S with $w/c=0.3$ and 0.4, respectively. Figure 2 also depicts the temporal evolution of $S(q,t)$ for D_2O hydrating C_3S with $w/c=0.3$. The time interval between two successive measurements was 5 min for all these measurements. Figure 3 depicts the temporal evolution of the Porod exponent $\eta(t)$ associated with power-law scattering $S(q,t)\sim q^{-\eta(t)}$, as estimated from $\ln[S(q,t)]$ vs $\ln(q)$, in the q range 0.00423–0.01659 $Å^{-1}$ for various H_2O and D_2O hydrating specimens. While $\eta(t)$ for all H_2O hydrating specimens lies in the range of 4.3–3.93, for D_2O hydrating specimen $\eta(t)$ starts from 4.187 decreasing for a while to a value of 4.09 at about 500 min, then rises to 4.5 at a time slightly greater than 2000 min and finally decreases monotonically, with different slopes, to 3.86 at about 4000 min.

It is important to note that the positive deviation of $\eta(t)$ from 4 is indicative of diffuse or fuzzy interface (23–26) of the gels. It is pertinent to note here that for fractals, η is less than 4. It can be as high as 8 for diffuse interface with sufficient width. Previously, positive deviation of η from the "classical" value of 4 has been observed[29–32] for various systems.

Figure 3 indicates that for H_2O hydrating specimens, the C-S-H gel has diffuse interface in the length scale of 10^2-10^3 Å (LS2) initially. As time progresses, the interface tends to become sharp and subsequently tends to have surface fractal morphology at about 1000 min after the onset of the hydration reaction. In contrast, for D_2O hydrating specimen, the temporal evolution of surface morphology of C-S-D gel has nonmonotonic nature. To begin with, the gel has diffuse interface but the width of the interface decreases initially before rising and finally coming down to have surface fractal morphology. From the above observations, we conclude that the temporal evolution of surface morphology of the gel, both for H_2O and D_2O hydrating cement, is strongly length-scale dependent. Based on the present and previous observations, Figs. 4 and 5 illustrate schematically the temporal evolution of mesoscopic structure for hydration of cement with H_2O and D_2O, respectively.

IV. CONCLUSIONS

In conclusion, present investigation enables us to outline the temporal evolution of the mesoscopic structure, at different length scales, of hydrating cement paste with H_2O and D_2O. It reveals that the structure exhibits temporal oscillations—strongly dependent on the scale of observation and on the medium of hydration. Sol-to-gel transition was observed for hydration with H_2O. While the formation of $Ca(OH)_2$ and C-S-H gel is synchronous for hydration with H_2O, the process appears to be nonsynchronous for hydration with D_2O. No conclusion could be drawn about the formation of $Ca(OD)_2$ at the onset of hydration with D_2O, but at later stages hydration proceeds with formation of insignificant amount of C-S-D and a relatively large amount of $Ca(OD)_2$.

The understanding as to why scaling is observed in hydration with H_2O and not with D_2O emerges as a natural consequence of this investigation. The morphology of the H_2O hydrating gel is a mass fractal with fractal dimension increasing with time initially and reaching a plateau. For hydration with D_2O, the gel changes topographically with time, unlike in the case of hydration with H_2O. In the beginning, the gel is ramified throughout the volume but the degree of ramification decreases with time. Subsequently, the mass transforms into objects with uniform internal density of unramified core with ramified surface showing self-similarity. Later, the ramified surface grows into ramified volume during hydration—the degree of ramification increasing with time. This topographical change in the hydrating mass as a function of time is one of the plausible reasons why scaling is not observed in the case of hydration with D_2O. Further, the formation rates of C-S-D and $Ca(OD)_2$ vary differently with time for hydration with D_2O. This is another reason why scaling is not observed for hydration with D_2O.

Mesoscopic structure of cement paste exhibits isotope effect. The structures arise from well-characterized chemical reactions as water diffuses through the porous material to bring about the water-surface interactions within the complex local geometry. The worth noting observations point to the effect of hydrogen bonding on mesoscopic structure resulting from hydration although hydrogen bond with deuterium is only slightly stronger than that with hydrogen.

ACKNOWLEDGMENTS

We are grateful to H. Stuhrmann, J. Zaccai, Steve King, U. D. Kulkarni, and other colleagues, who have reviewed the manuscript, for many useful suggestions. S.M. thankfully acknowledges financial support received from DST, India through S. N. Bose Institute, Kolkata, India for experimental work at LLB, Saclay, France.

APPENDIX

Model Calculation-I. Dealing with effect of changing coherence characteristic of inhomogeneities on $S(0,t)$. Let us consider a model system with one inhomogeneity with total scattering length ζ at time t. At time $t+\delta$, the inhomogeneity transforms into two inhomogeneities with total scattering length $(\zeta-\alpha)$ and α, respectively, following the conservation of total scattering length. For the convenience of discussion, to begin with we assume that both α and ζ are positive—a case pertinent for hydration with D_2O as C_3S, D_2O, C-S-D, and $Ca(OD)_2$ all have positive scattering length densities. The hydration with H_2O will be dealt with in a subsequent discussion. scattering length densities for C_3S, $Ca(OH)_2$, $Ca(OD)_2$, and D_2O are 3.94×10^{14} m^{-2}, 1.6×10^{14} m^{-2}, 5.33×10^{14} m^{-2}, and 6.365×10^{14} m^{-2}, respectively. For the aforementioned model system, $S(0,t+\delta)-S(0,t)=[(\zeta-\alpha)^2+\alpha^2-\zeta^2]=2\alpha(\alpha-\zeta)\leq 0$, since $\alpha\leq\zeta$. Case-I signifies splitting of a macrodomain into smaller domains can only cause reduction in $S(0,t)$ with t. On the contrary when two or more inhomogeneities having positive scattering length densities join together to form a coherent mass, $S(0,t+\delta)-S(0,t)\geq 0$. A contiguous domain having uniform chemical composition and hence uniform scattering length density is termed as coherent mass. Composition modulation leads to incoherence. Scattering centers within a coherent mass scatter coherently.

Conclusions will just reverse when α and ζ are of opposite sign. This case is pertinent for hydration of cement with H_2O as it has negative scattering length density. Scattering length density for H_2O is -0.5589×10^{14} m^{-2}. For two inhomogeneities with opposite sign of scattering length densities α and $(\zeta-\alpha)$ join together to form a coherent mass, $S(0,t+\delta)-S(0,t)=2\alpha(\zeta-\alpha)\leq 0$. Considering the fact that H_2O has negative scattering length density, a domain of C-S-H phase can have both positive and negative scattering length densities depending on H_2O content in the phase. As hydration proceeds, a domain of C-S-H gel can phase separates into two of more domains of varying composition from each other. Contact with H_2O and/or with unreacted C_3S can lead to the phase splitting of a C-S-H domain caused by diffusion of H_2O. The following possibilities are relevant. (I.i) For $\zeta>0$ and $\alpha<0$, for the case of domain splitting $S(0,t+\delta)-S(0,t)=2\alpha(\alpha-\zeta)>0$. (I.ii) For $\zeta<0$ and $\alpha>0$, for the case of domain splitting $S(0,t+\delta)-S(0,t)=2\alpha(\alpha-\zeta)>0$. (I.iii) For $\zeta<0$ and $\alpha<0$, for the case of domain splitting $S(0,t+\delta)-S(0,t)=2\alpha(\alpha-\zeta)>0$ for $|\alpha|>|\zeta|$ and $S(0,t+\delta)-S(0,t)=2\alpha(\alpha-\zeta)<0$ for $|\alpha|<|\zeta|$.

Model Calculation-II. Dealing with effect of extent of hydration reaction with D_2O on $S(0,t)$. Let us consider a model system containing reactant mixture of one C_3S particle with total scattering length ζ_c reacting with one domain of D_2O with total scattering length ζ_w at time t. At time $t+\delta$, the reactant mixture transforms into unreacted C_3S particle with total scattering length $(\zeta_c-\alpha)$, domain of free water with total scattering length $(\zeta_w-\beta)$, $Ca(OD)_2$ particle with total scattering length density γ and hydrated gel C-S-D with total scattering length $(\alpha+\beta-\gamma)$, respectively, following the conservation of total scattering length. As discussed before, C-S-D has variable stoichiometry and hence has variable mass density and scattering length density. However, ω_3 the ratio between mass density and scattering length density of C-S-D bears a simple relation $\omega_3=(\alpha\omega_1+\beta\omega_2-\gamma\omega_4)/(\alpha+\beta-\gamma)$ following mass-conservation law in the aforementioned chemical reaction where ω_1, ω_2, and ω_4 are, respectively, the ratios between mass densities and scattering length densities of C_3S, D_2O, and $Ca(OD)_2$.

For the aforementioned model system, $S(0,t+\delta)-S(0,t)=[(\zeta_c-\alpha)^2+(\zeta_w-\beta)^2+(\alpha+\beta-\gamma)^2+\gamma^2-\zeta_c^2-\zeta_w^2]=2[\alpha(\alpha-\zeta_c)+\beta(\beta-\zeta_w)+\alpha\beta-\gamma(\alpha+\beta-\gamma)]$ with α, β, $\gamma\geq 0$, $(\alpha+\beta)\geq\gamma$, $\gamma(\alpha+\beta-\gamma)\geq 0$, $\alpha\leq\zeta_c$, $\beta\leq\zeta_w$, $\zeta_c>0$, and $\zeta_w>0$ for hydration of cement with D_2O. Now let us consider few pertinent cases:

(II.i) For $\alpha\ll\zeta_c$ and $\beta\ll\zeta_w$, $S(0,t+\delta)-S(0,t)\approx 2[\alpha\beta-\alpha\zeta_c-\beta\zeta_w-\gamma(\alpha+\beta-\gamma)]$. Now let us consider three possibilities. If $\zeta_c=\zeta_w$,

$$\begin{aligned}S(0,t+\delta)-S(0,t)&\approx 2[\alpha\beta-\alpha\zeta_c-\beta\zeta_w-\gamma(\alpha+\beta-\gamma)]\\&=2[\alpha\beta-\alpha\zeta_c-\beta\zeta_c-\gamma(\alpha+\beta-\gamma)]\\&=2[\beta(\alpha-\zeta_c)-\alpha\zeta_c-\gamma(\alpha+\beta-\gamma)]<0\end{aligned}$$

since $\alpha\leq\zeta_c$. For $\zeta_c>\zeta_w$,

$$\begin{aligned}S(0,t+\delta)-S(0,t)&\approx 2[\alpha\beta-\alpha\zeta_c-\beta\zeta_w-\gamma(\alpha+\beta-\gamma)]\\&=2[\alpha(\beta-\zeta_c)-\beta\zeta_w-\gamma(\alpha+\beta-\gamma)]<0\end{aligned}$$

since $\zeta_c>\zeta_w\gg\beta$. For $\zeta_c<\zeta_w$,

$$\begin{aligned}S(0,t+\delta)-S(0,t)&\approx 2[\alpha\beta-\alpha\zeta_c-\beta\zeta_w-\gamma(\alpha+\beta-\gamma)]\\&=2[\beta(\alpha-\zeta_w)-\alpha\zeta_c-\gamma(\alpha+\beta-\gamma)]<0\end{aligned}$$

since $\zeta_w>\zeta_c\gg\alpha$. The conclusion remains unchanged even for $\gamma=0$, i.e., irrespective of formation of $Ca(OD)_2$.

So for $\alpha\ll\zeta_c$ and $\beta\ll\zeta_w$, $S(0,t+\delta)-S(0,t)<0$ signifying decay of $S(0,t)$ with t for a slow reaction irrespective of formation of $Ca(OD)_2$. (II.ii) For $\alpha=0$ and $\beta=0$, $S(0,t+\delta)-S(0,t)=0$ signifying static nature of $S(0,t)$ for no reaction. (II.iii) For a fast reaction or for long elapsed reaction time when $\alpha\approx\zeta_c$ and $\beta\approx\zeta_w$, $S(0,t+\delta)-S(0,t)\approx 2[\alpha\beta-\gamma(\alpha+\beta-\gamma)]$. The following cases are pertinent:

(II.iii.A) For $\alpha=\gamma$ or $\beta=\gamma$, $S(0,t+\delta)-S(0,t)=0$. (II.iii.B) For $\alpha=\beta\neq\gamma$, $S(0,t+\delta)-S(0,t)>0$. (II.iii.C) For $\alpha>\beta>\gamma$ and $\beta>\alpha>\gamma$, $S(0,t+\delta)-S(0,t)>0$. (II.iii.D) For $\alpha>\gamma>\beta$ and $\beta>\gamma>\alpha$, $S(0,t+\delta)-S(0,t)<0$. (II.iii.E) For $\gamma\approx 0$, $S(0,t+\delta)-S(0,t)>0$ signifying growth of $S(0,t)$ for fast reaction or long elapsed reaction time with negligible production of $Ca(OD)_2$; (II.iii.F) For $(\alpha+\beta-\gamma)\approx 0$, $S(0,t+\delta)-S(0,t)>0$ signifying growth of $S(0,t)$ for fast reaction or long elapsed reaction time with negligible production of C-S-D.

(II.iv) For $\alpha\approx\zeta_c$ only, $S(0,t+\delta)-S(0,t)=2[\beta(\zeta_c+\beta-\zeta_w)-\gamma(\alpha+\beta-\gamma)]=2[\beta(\alpha+\beta-\zeta_w)-\gamma(\alpha+\beta-\gamma)]$. So the relative values of β $(\alpha+\beta)$ and $[\zeta_w+\gamma(\alpha+\beta-\gamma)]$ determine growth or decay of $S(0,t)$. By similarity argument, for $\beta\approx\zeta_w$ only, the relative values of $\alpha(\alpha+\beta)$ and $[\zeta_c+\gamma(\alpha+\beta-\gamma)]$ determine growth or decay of $S(0,t)$.

Model Calculation-III. Dealing with effect of extent of hydration reaction with H_2O on $S(0,t)$. Let us consider a model system containing reactant mixture of one C_3S particle with total scattering length ζ_c reacting with one domain of H_2O with total scattering length ζ_w at time t. At time $t+\delta$, the reactant mixture transforms into unreacted C_3S particle with total scattering length $(\zeta_c-\alpha)$, domain of free water with total scattering length $(\zeta_w-\beta)$, $Ca(OH)_2$ particle with total scattering length density γ and hydrated gel C-S-H with total scattering length $(\alpha+\beta-\gamma)$, respectively, following the conservation of total scattering length. As discussed before, C-S-H has variable stoichiometry and hence has variable mass density and scattering length density. Scattering length density $(\alpha+\beta-\gamma)$ of C-S-H gel can assume both negative and positive values depending upon the H content. For the present model system,

$$S(0,t+\delta) - S(0,t) = [(\zeta_c-\alpha)^2 + (\zeta_w-\beta)^2 + (\alpha+\beta-\gamma)^2 + \gamma^2 - \zeta_c^2 - \zeta_w^2] = 2[\alpha(\alpha-\zeta_c) + \beta(\beta-\zeta_w) + \alpha\beta - \gamma(\alpha+\beta-\gamma)]$$

with α, $\gamma \geq 0$, $\beta \leq 0$, $\zeta_c > 0$, $\zeta_w < 0$, $\alpha \leq \zeta_c$, $\beta \geq \zeta_w$, and $\gamma(\alpha+\beta-\gamma)$ can assume both positive and negative values depending on composition of C-S-H. Further, $2[\alpha(\alpha-\zeta_c)+\beta(\beta-\zeta_w)+\alpha\beta] \leq 0$ as $\zeta_c > 0$, $\zeta_w < 0$, $\alpha \geq 0$, $\alpha \leq \zeta_c$, $\beta \leq 0$, and $\beta \geq \zeta_w$ indicating temporal decay of $S(0,t)$ for hydration of cement with H_2O when $Ca(OH)_2$ formation is negligibly small, i.e., $x \approx 3$ or $\gamma \approx 0$. However, when $Ca(OH)_2$ formation is not negligibly small and $\gamma(\alpha+\beta-\gamma)$ assumes positive value for $(\alpha+\beta-\gamma) > 0$, $S(0,t)$ will decay with time. This case is pertinent when C-S-H gel phase is cement rich. For period when C-S-H gel phase is water rich, $S(0,t)$ can grow with time.

*Author to whom correspondence should be addressed; smazu@barc.gov.in

[1] J. W. Cahn, Acta Metall. **9**, 795 (1961).
[2] A. J. Bray, Adv. Phys. **43**, 357 (1994), and references therein.
[3] S. Mazumder, D. Sen, A. K. Patra, S. A. Khadilkar, R. M. Cursetji, R. Loidl, M. Baron, and H. Rauch, Phys. Rev. Lett. **93**, 255704 (2004).
[4] S. Mazumder, D. Sen, A. K. Patra, S. A. Khadilkar, R. M. Cursetji, R. Loidl, M. Baron, and H. Rauch, Phys. Rev. B **72**, 224208 (2005).
[5] S. Mazumder, Physica B **385-386**, 7 (2006).
[6] S. Mazumder, R. Loidl, and H. Rauch, Phys. Rev. B **76**, 064205 (2007).
[7] D. Sen, S. Mazumder, and J. Bahadur, Phys. Rev. B **79**, 134207 (2009).
[8] B. Mandelbrot, *The Fractal Geometry of Nature* (Freeman, San Francisco, 1982); J. Feder, *Fractals* (Plenum, New York, 1988).
[9] H. L. Le Chatelier, *Experimental Researches on the Constitution of Hydraulic Mortars* (McGraw-Hill, New York, 1905).
[10] H. F. W. Taylor, *Cement Chemistry* (Academic Press, London, 1990).
[11] Z. Xu and D. Viehland, Phys. Rev. Lett. **77**, 952 (1996).
[12] I. G. Richardson and G. W. Groves, Cem. Concr. Res. **22**, 1001 (1992).
[13] H. F. W. Taylor, J. Am. Ceram. Soc. **69**, 464 (1986).
[14] S. A. Greenberg, T. N. Chang, and E. Andersen, J. Phys. Chem. **64**, 1151 (1960).
[15] S. A. Greenberg and T. N. Chang, J. Phys. Chem. **69**, 182 (1965).
[16] K. Fujii and W. Kondo, J. Am. Ceram. Soc. **66**, C-220 (1983).
[17] M. Kriechbaum, G. Degovics, P. Laggner, and J. Tritthart, Adv. in Cement Res **6**, 93 (1994).
[18] A. Heinemann, H. Hermann, K. Wetzig, F. Häussler, H. Baumbach, and M. Kröning, J. Mater. Sci. Lett. **18**, 1413 (1999).
[19] M. Kriechbaum, G. Degovics, J. Tritthart, and P. Laggner, Prog. Colloid Polym. Sci. **79**, 101 (1989).
[20] T. C. King, C. M. Dobson, and S. A. Rodger, J. Mater. Sci. Lett. **7**, 861 (1988).
[21] G. C. Bye, *Portland Cement: Composition, Production and Properties* (Pergamon Press, Oxford, 1983).
[22] D. P. Bentz, P. V. Coveney, E. J. Garboczi, M. F. Kleyn, and P. E. Stutzman, Modell. Simul. Mater. Sci. Eng. **2**, 783 (1994), and also http://ciks.cbt.nist.gov/garbocz/cell1994/node4.htm
[23] S. Mazumder, D. Sen, T. Saravanan, and P. R. Vijayaraghavan, J. Neutron Res. **9**, 39 (2001).
[24] M. Hainbuchner, M. Villa, G. Kroupa, G. Bruckner, M. Baron, H. Amenitsch, E. Seidl, and H. Rauch, J. Appl. Crystallogr. **33**, 851 (2000).
[25] L. Van Hove, Phys. Rev. **95**, 249 (1954).
[26] F. M. Lea, *Chemistry of Cement and Concrete*, 4th ed. (Elsevier Science & Technology, New York, 2004).
[27] R. B. Williamson, Prog. Mater. Sci. **15**, 189 (1972).
[28] Wikipedia (Wikimedia Foundation Inc.), Heavy water, http://en.wikipedia.org/wiki/Heavy_water
[29] S. Mazumder, D. Sen, I. S. Batra, R. Tewari, G. K. Dey, S. Banerjee, A. Sequeira, H. Amenitsch, and S. Bernstorff, Phys. Rev. B **60**, 822 (1999).
[30] R. Tewari, S. Mazumder, I. S. Batra, G. K. Dey, and S. Banerjee, Acta Metall. **48**, 1187 (2000).
[31] P. W. Schmidt, D. Avnir, D. Levy, A. Höhr, M. Steiner, and A. Röll, J. Chem. Phys. **94**, 1474 (1991).
[32] U. Dahlborg, M. C. Dahlborg, P. S. Popel, and V. E. Sidorov, Eur. Phys. J. B **14**, 639 (2000).